Electronic and atomic structure of thin $CoSi_2$ films on Si(111) and Si(100)

D. D. Chambliss* and T. N. Rhodin
School of Applied and Engineering Physics, Cornell University, Ithaca, New York 14853

J. E. Rowe
AT&T Bell Laboratories, Murray Hill, New Jersey 07974

(Received 27 March 1991)

The electronic and atomic structure of very thin epitaxial cobalt silicide films was studied to provide insight into the initial stages of interface formation. Thin $CoSi_2$ films (3–30 Å) on Si(111) and Si(100) were studied experimentally using angle-resolved photoemission spectroscopy, low-energy electron diffraction (LEED), and Auger electron spectroscopy, and computationally using the pseudofunction method of Kasowski for determining the electronic band structure. The experimental and computational results support the models of Hellman and Tung for Co-rich and Si-rich $CoSi_2$(111) surfaces. The surface-state dispersion that we measure for the Co-rich variant agrees with the behavior that we calculate for the Hellman-Tung model. For the Si-rich variant, the essentially bulklike bonding environment of the outermost Co atoms in the Hellman-Tung model agrees with the photoemission results. Preliminary results for thin films of $CoSi_2$ on Si(100) grown by a template technique show clearly a strong dependence of film quality on the annealing temperature and initial Co thickness. A model for surface structure is suggested that accounts for LEED and photoemission results.

I. INTRODUCTION

The closely related crystal structures and very small lattice mismatch between Si and $CoSi_2$ makes Si-$CoSi_2$ interfaces important both for their technological possibilities[1] and for the study of metal-semiconductor interfaces that are structurally nearly ideal. It has long been known that, under UHV conditions, $CoSi_2$ can be grown on Si(111) surfaces to form nearly perfect uniform epitaxial thin films.[1,2] High-quality epitaxy of $CoSi_2$ on Si(100) is a more recent development.[3–5] The electronic and atomic structure of the surfaces of $CoSi_2$ films on Si is important for technological applications of these films because the surface structures impose significant constraints on the growth of thicker films. Furthermore, an understanding of the bonding trends at these surfaces may facilitate better film growth through temperature and deposition control and controlled introduction of impurities to determine surface structure.

Considerable effort has gone into understanding the bulk, interface, and surface properties of $CoSi_2$ on Si(111). The electronic structure of bulk $CoSi_2$ has been studied with band-structure calculations,[6,7] which are largely in agreement with de Haas–van Alphen measurements on bulk samples.[8] Valence-band photoemission experiments on epitaxial films[9–11] are substantially in agreement with computed band structure, although photoemission features associated with less-strongly-hybridized Co($3d$) states have energy somewhat closer to the Fermi level E_F than calculated energies for the corresponding one-electron levels. This discrepancy has been attributed to the inadequacy of using one-electron energy levels for describing photoemission from localized orbitals.[9] The dominant features in the density of states are a peak due to nonbonding Co($3d$) states at about -2.0 eV (relative to E_F) and a peak due to bonding Co($3d$)-Si($3p$) hybrids at about -4.0 eV.

It has been found that different preparations of epitaxial $CoSi_2$(111) films yield different surface structures with distinctive low-energy electron diffraction (LEED) and photoemission behavior.[11] For films prepared by deposition of Co followed by annealing, a low-temperature (420 °C) anneal produces a cobalt-rich "$CoSi_2$-Co" surface, and annealing above 550 °C yields the silicon-rich "$CoSi_2$-Si" surface. Hellman and Tung[12] found that $CoSi_2$-Co could be transformed to $CoSi_2$-Si by the deposition of two monolayers (ML's) of Si, and the $CoSi_2$-Co surface could be recovered by depositing 1 ML of Co on $CoSi_2$-Si and annealing. The two surfaces have different photoemission behavior, and in particular the $CoSi_2$-Co surface has two surface states, one dispersive and one nondispersive, that are not found on $CoSi_2$-Si.[11] To account for this difference Pirri *et al.* suggested that $CoSi_2$-Co and $CoSi_2$-Si are bulklike $CoSi_2$ structures truncated just above and just below a plane of Co atoms, as shown in Figs. 1(a) and 1(b). On the other hand, the models shown in Figs. 1(c) and 1(d), which contain one more monolayer of Si than those of Figs. 1(a) and 1(b), seem to agree better with measured Auger peak ratios,[12] LEED I-V measurements,[13] medium-energy ion scattering,[14] and Auger electron diffraction in $CoSi_2$ clusters grown with relatively low Co coverage.[15] Core-level photoemission studies[16] have presented two different interpretations but are both qualitatively consistent with the model of Figs. 1(c) and 1(d). The question, then, is whether the observed valence-band photoemission results, particularly the surface states, are consistent with the models of Figs. 1(c) and 1(d), in which the outermost Co atoms are in a nearly bulklike environment with bonds to seven Si neighbors.

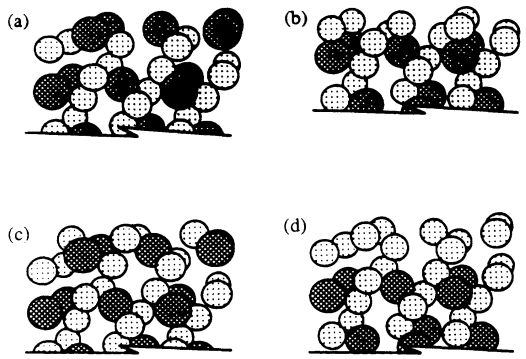

FIG. 1. Models for $CoSi_2(111)$ surfaces. Perspective view looks roughly along the $[\bar{1}10]$ direction. (a) $CoSi_2(111)$-Co model of Pirri *et al.* (Ref. 11). (b) $CoSi_2(111)$-Si model of Pirri *et al.* (c) $CoSi_2(111)$-Co model of Hellman and Tung (Ref. 12). (d) $CoSi_2(111)$-Si model of Hellman and Tung.

While epitaxial $Si(111)/CoSi_2(111)$ interfaces of high quality are relatively easy to produce, conduction through an ideal (111) interface is expected to be poor because there are no electronic states in $CoSi_2$ matching energy and parallel momentum with states near the Si conduction-band minimum.[16] $Si(100)/CoSi_2(100)$ interfaces, on the other hand, are expected to have these matching states, so there is great interest in achieving and understanding high-quality epitaxy with this orientation. Epitaxial growth of $CoSi_2$ on Si(100) has only recently been reported. Depositing a thick Co layer (>200 Å) and annealing it, which on Si(111) can produce high-quality epitaxy, on Si(100) yields a $CoSi_2$ layer with grains of many orientations.[3] A template growth method, however, allows $CoSi_2$ to grow epitaxially on Si(100) with two dominant orientations: $CoSi_2(100)$ and $CoSi_2(110)$.[4,5] This technique is to deposit 2 Å of Co at room temperature and to anneal the sample at 450 °C. The proportion of (100) and (110) grains is very sensitive to the topography of the substrate. Other recipes involving Si deposition can produce films of predominantly one orientation. Once a template layer is established, thicker $CoSi_2$ films grown by depositing Co and Si in the atom ratio [Co]:[Si]=1:2 followed by annealing tend to follow the crystal orientations established in the template. As on Si(111), $CoSi_2$ films on the Si(100) can have cobalt-rich or silicon-rich surfaces, with clearly different LEED patterns.[4] Samples with different fractions of (100) and (110) grains, resulting from different preparations conditions, do not exhibit markedly different LEED patterns.

We have studied the formation and surface structures of thin $CoSi_2$ layers on Si(111) and Si(100) by performing angle-resolved ultraviolet photoemission spectroscopy (ARUPS) experiments. The experimental results are analyzed by comparison with *ab initio* calculations of electronic band structure for proposed atomic configurations. This close coupling of experiment with calculations provided a powerful approach to understanding surface atomic and electronic structure. By this means the photoemission behavior confirmed the structural model for $CoSi_2(111)$ supported by several other studies. For $CoSi_2(100)/Si(100)$ the uncertainties in sample preparation make interpretation somewhat more problematic. The photoemission results are sensitive to details of annealing temperature and initial Co coverage. A model is proposed that helps to explain the LEED and photoemission results. Comparison with calculations shows further that the effects of finite film thickness may also be important to understanding the spectra.

II. EXPERIMENTAL PROCEDURES

The experiments were performed on the *U4A* beam line of the National Synchroton Light Source at Brookhaven National Laboratory. Samples were prepared in a preparation chamber with base pressure 2×10^{-10} Torr and transferred in vacuum to an analysis chamber for photoemission studies. Silicon samples were cleaned with cycles of neon-ion bombardment (ion energy 1 keV) and heating to 800 °C–900 °C by electron bombardment. The sample temperature was measured using an infrared pyrometer. Auger spectroscopy (single-pass cylindrical mirror analyzer; $E_{\rm pri}=3$ keV, $V_{\rm mod}=2V_{p\text{-}p}$) was used to verify cleanliness, with peak-to-peak ratios $I(C_{KLL})/I(Si_{LVV})$ of at most 0.01 and typically 0.002 and $I(O_{KLL})/(Si_{LVV})<0.0003$. The LEED patterns of the Si(111) and Si(100) substrates were (7×7) and (2×1) patterns, respectively, characteristic of clean, well-ordered Si surfaces.

Cobalt layers of thickness 0.1–10 Å were deposited at approximately 0.5 Å/min by sublimation from a Co target attached to a tungsten plate and heated by electron bombardment to 1240 °C, monitored with a W/(W-Re) thermocouple on the front Co surface. The sublimator was contained in a collimating LN_2 cryoshroud equipped with a shutter. Immediately after typical depositions lasting approximately 5 min, the chamber pressure was measured at $(3-5)\times10^{-10}$ Torr. The deposition rate was estimated with a quartz crystal thickness monitor and calibrated afterward using relative Auger peak heights and *ex situ* Rutherford backscattering (RBS) measurements. RBS and Auger results confirmed that this deposition procedure produced cobalt coverages reproducible to 10%. The system was also equipped for deposition of silicon by evaporation from a tantalum crucible, heated by electron bombardment. The pressure rise during Si evaporation was typically $<1\times10^{-10}$ Torr. This allowed conversion between Co- and Si-rich variants of $CoSi_2$ surfaces by titration with Co or Si, so that their electronic differences could be probed. Although Si-rich surfaces can be produced by using a higher annealing temperature,[11] the high temperature can also cause morphological changes that could affect photoemission results so Si deposition is superior. The Si-deposition rate was calibrated using the transition from $CoSi_2(111)$-Co to $CoSi_2(111)$-Si, as observed with LEED. This involved significant uncertainty. Most samples were annealed after Co deposition; temperatures below 600 °C (the lower limit of pyrometer accuracy) were estimated by measuring temperature as a function of heater power and extrapolating toward lower temperatures. This extrapolation

adds about ±20 °C to the uncertainty in temperature measurement.

The rotatable hemispherical analyzer was typically operated to give an overall energy resolution of $\Delta E \leq 0.1$ eV full width at half maximum (FWHM) and an angle resolution of $\Delta\theta \approx 1°$ FWHM. It was observed that the instrumental response function of the analyzer did not have a typical Gaussian shape, but had a less sharp drop-off. This has the effect that the Fermi-edge cutoff is broader than the FWHM suggests. The energy resolution of photons from the toroidal grating monochromator was generally $\Delta h\nu \leq 0.05$-eV FWHM for ARUPS spectra.

III. ELECTRONIC AND ATOMIC STRUCTURE OF $CoSi_2$/Si(111)

A. Photoemission experiments

$CoSi_2$ film samples of comparable thickness were prepared with different free surfaces, namely $CoSi_2$-Co and $CoSi_2$-Si. The more Si-rich samples were grown by depositing 2-Å Co followed by approximately 5-Å Si on a Si(111) substrate at room temperature and annealing to 450 °C. A more cobalt-rich sample was prepared by depositing another 1-ML Co on a Si-rich sample and annealing again at 450 °C. The cobalt-rich or silicon-rich character of these films was determined by comparing Auger peak ratios and the energy dependence of the (1×1) LEED patterns with the results of Hellman and Tung.[12] The results indicate that the Co-rich sample is predominantly $CoSi_2$-Co, while the Si-rich sample is approximately half $CoSi_2$-Si and half $CoSi_2$-Co.

The Si-rich and Co-rich samples have quite different photoemission behavior, as seen in Fig. 2(a). At these photon energies the spectra primarily reveal the density of states near the surface rather than bulklike band structure. The silicon-rich surface yields a smaller Co(3d) contribution relative to the inelastic background than the cobalt-rich surface, as expected in the presence of an additional Si bilayer at the surface. Furthermore, the peak positions are different. For the silicon-rich surface the spectra at high photon energy agree with both the calculated density of states for bulk $CoSi_2$ (Ref. 6) and with bulk band dispersions measured using photoemission.[9] The largest peaks are close to the L_1 band minimum at −2.05 eV. This suggests that even the outermost Co in the silicon-rich surface sees a bulklike bonding environment. The cobalt-rich surface is a markedly different environment, and the peak is about 0.6 eV higher in energy.

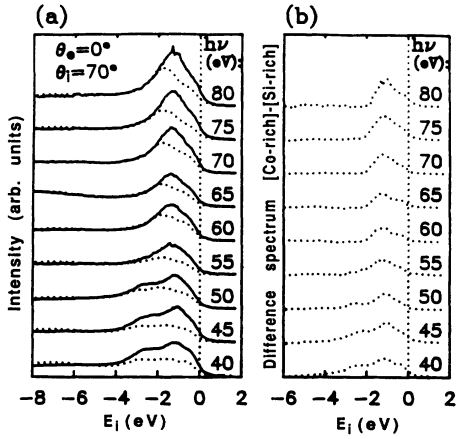

FIG. 2. Difference in electronic structure between $CoSi_2$(111)-Si and $CoSi_2$(111)-Co surfaces. (a) Normal-emission ARUPS spectra from $CoSi_2$-Co (solid curves) and $CoSi_2$-Si (dotted curves). Spectra are scaled so the intensities at $E_i < -4$ eV match. The shoulder at −2.8 eV for photon energies ≤ 50 eV is indicative of the $CoSi_2$-Co surface. (b) Differences between spectra from cobalt-rich and silicon-rich samples. Difference curves above $h\nu = 55$ eV are essentially identical and represent the surface density of states of the $CoSi_2$-Co surface.

To investigate the differences further it is useful to consider the difference spectra shown in Fig. 2(b). The difference spectra have the same shape as the Co(3d) features in the silicon-rich spectra, but shifted to higher energy (i.e., toward E_F) by 0.7 eV. This suggests that the cobalt-rich spectra are simply the superposition of the silicon-rich spectra and distinct additional emission from the added surface Co. It might be supposed that the large difference between the densities of state at the surface and the bulk would weigh against the silicon-terminated model for $CoSi_2$(111)-Co [Fig. 1(c)], whose sevenfold coordination seems "nearly bulklike." Explicit calculations, discussed below, show that this intuitive conclusion is not valid, for the silicon-terminated model in fact best explains the ARUPS results.

Near $h\nu = 45$ eV, the dispersive surface state reported by Pirri *et al.*[10] is apparent at $E_i = -2.8$ eV. This peak is sensitive to the photon vector potential normal to the surface ($A_\perp$) and thus has Λ_1 symmetry. It is not seen in spectra from samples annealed at > 600 °C to produce a silicon-rich surface. Its presence on the Si-rich sample confirms that this surface was not entirely $CoSi_2$-Si. The dispersion of the surface state along the $\bar{\Gamma}$–$\bar{M}$ line in the surface Brillouin zone was measured using off-normal-emission spectra from several samples and is shown in Fig. 3. Also shown in Fig. 3 are the locations of other peaks and shoulders in these spectra, which include a second nearly dispersionless surface state at −1.4 eV with Λ_3 symmetry at $\bar{\Gamma}$, and some structure near E_F not clearly resolved as true surface-state behavior.[10]

The effects of film thickness on electronic structure were examined by depositing different thicknesses of Co onto a substrate heated at 450±30 °C. These samples also exhibited (1×1) LEED patterns. Co coverage of 1, 2, and 10 ML were used to produce $CoSi_2$ layers of average thickness 3.1, 6.3, and 31 Å. The Auger peak height ratios suggest that the low annealing temperature produced $CoSi_2$-Co surfaces. Although aggregation of $CoSi_2$ into thicker islands can occur at these Co coverages when a higher annealing temperature is used,[15] it is clear from the Auger peak ratios that this did not occur in these samples. The low intensity in the ARUPS spectra of the peak around −7 eV, originating in bulk-silicon density of states, confirms that significant areas of Si were not exposed.

Photoemission spectra from these films (Fig. 4) illus-

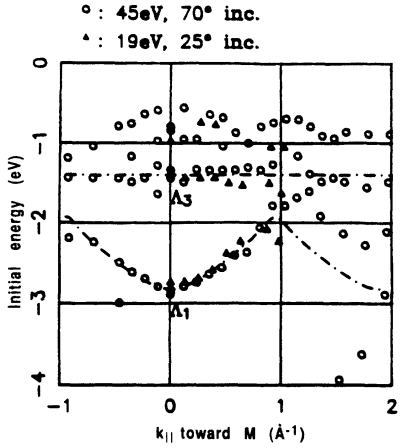

FIG. 3. Dispersion of the surface states of the $CoSi_2$(111)-Co surface. Dispersion along the $\bar{\Gamma}-\bar{M}$ line in the surface Brillouin zone is measured using photon energies of 45 eV (circles) and 19 eV (triangles). Dashed lines suggest dispersion of states with Λ_1 and Λ_3 symmetry. Features at higher energy arise from bulk bands.

trate how the discrete states of a $CoSi_2$ film with only one or two Co layers (3.1 or 6.3 Å) differ from the bulklike band structure (represented by the 31-Å film). The features in the 6.3-Å spectra are similar to those from the thick film but less sharply defined. The thinnest film,

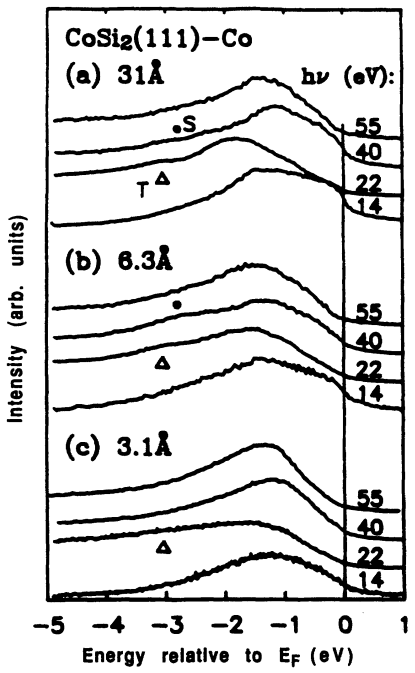

FIG. 4. Normal-emission photoemission spectra from $CoSi_2$ films of different thicknesses on Si(111) at representative photon energies. (a) 31-Å $CoSi_2$ film. (b) 6.3-Å film. (c) 3.1-Å film. Incidence angle is 70° at 55 and 40 eV, 25° at 22 and 14 eV. Solid circles mark surface state S of Λ_1 symmetry; triangles mark feature T.

however, is quite different, particularly in the low intensity of emission near E_F. The Λ_1 surface state is not seen for the thinnest film. Thus the quantization of Λ_1-symmetry states is different in a single $CoSi_2$ layer from both bulk and surface $CoSi_2$(111). There appears for these samples a broad feature T with $E_i = -3.0$ eV. While T is close in energy to the Λ_1 surface state discussed above, it is $A_{\|}$ -sensitive and thus of different symmetry and its photon-energy variation is different. The 6.3- and 31-Å samples also displayed the Λ_1-surface state in other spectra. The behavior of T varied somewhat from sample to sample; it might thus be associated with defects at the surface or interface, or with small variations in film thickness and uniformity.

The photoemission results suggest a number of conclusions. The difference between silicon-rich and cobalt-rich (111) surfaces of $CoSi_2$ is clearly illustrated. The silicon-rich surface has a photoemission signature similar to bulk $CoSi_2$. This is what one would expect for the structure of Fig. 1(d), though other structures cannot be ruled out. The cobalt-rich spectra contain additional intensity which can be attributed to a surface layer in which the Co has not attained a bulklike disilicide bonding configuration. Yet an interpretation in terms of particular surface structures would be incomplete without the calculations of electronic structure that follow.

B. Comparison with calculations

The electronic structure for model atomic structures was computed within the local density approximation (LDA) using the pseudofunction method developed by Kasowski *et al.*,[17] and was compared with photoemission results for structural identification. The pseudofunction method has proved effective in computations on a range of problems, including bulk and surface properties of semiconductors.[17,18] The basis functions used in the pseudofunction method are similar to muffin-tin orbitals, but the radial functions for the basis set can be chosen with more freedom. Here the radial functions included sections of the true radial solution to the spherical potential derived in the self-consistent loop, so the basis itself responded to changes in the potential-energy function, even outside the muffin-tin spheres. The basis set included 7 functions per Si atom ($3s$ and $3p^3$ states plus three higher-energy p functions to increase the variational freedom) and 16 functions per Co atom ($4s$ and $3d^5$ states plus higher-energy s, p, and d functions). Sampling of the irreducible wedge of the two-dimensional Brillouin zone corresponded to an evenly spaced grid of 27 points in the full surface Brillouin zone. The Fourier expansions defining the pseudofunctions included all plane waves with energy < 10.6 Ry (1 Ry = 13.605 eV). Augmentation energies were chosen so that the logarithmic derivative of the wave function at the muffin-tin radius was slightly negative.

The models for $CoSi_2$(111) surfaces shown in Figs. 1(a), 1(c), and 1(d) were represented in calculations by the three slab structures shown in Fig. 5. [Calculations were not performed for the model of Fig. 1(b) because the singly bonded outermost Si atom is chemically implausible.]

Each model has three layers of Co atoms: two "surface" layers (top and bottom), which are like the outermost Co layer of the corresponding surface, and one "bulk" layer whose local environment is like bulk $CoSi_2$. Bulklike atom locations were assumed in Figs. 5(a) and 5(b); the most silicon-rich model, Fig. 5(c), used the inward relaxation measured by medium-energy ion scattering[14] for the outer Si bilayer and bulk sites for the remainder. Specific atomic models of Si-rich and Co-rich $CoSi_2$(100) surfaces have not yet been established to the point where band-structure modeling is likely to yield a confirmation of surface structure. Nonetheless, calculations were performed for Co-terminated and Si-terminated truncated-bulk $CoSi_2$(100) slabs with three Co layers to investigate the effect of the finite film thickness on the quantization of electronic states.

In comparing photoemission experiments with computed band structure it is essential to consider the accuracy to which the calculations can be expected to model photoemission results. There are three main sources of uncertainty: the LDA, approximation intrinsic to the pseudofunction method, and the approximate nature of the atomic models used. The LDA is not rigorously valid for predicting photoemission results, but LAPW-method calculations for bulk $CoSi_2$ (Ref. 6) agree with the photoemission measurements performed here within 0.2–0.4 eV (Table I). The limited basis set of the pseudofunction method as used here introduces additional errors and for bulk $CoSi_2$ it overestimates the Co($3d$) bonding-nonbonding energy difference in $CoSi_2$ by 50% as compared with the LAPW calculations.[19] This could be improved by introducing additional basis functions but this accuracy is sufficient for the comparisons made here. Since atomic models only approximately nine layers thick are used here, the bulk band structure is not fully developed. Nonetheless, careful analysis of results on the basis of symmetry and concentration of electronic charge allows the surface states to be identified. Comparison of experimental results with these calculations permits more definite conclusions than would be possible from experiments alone.

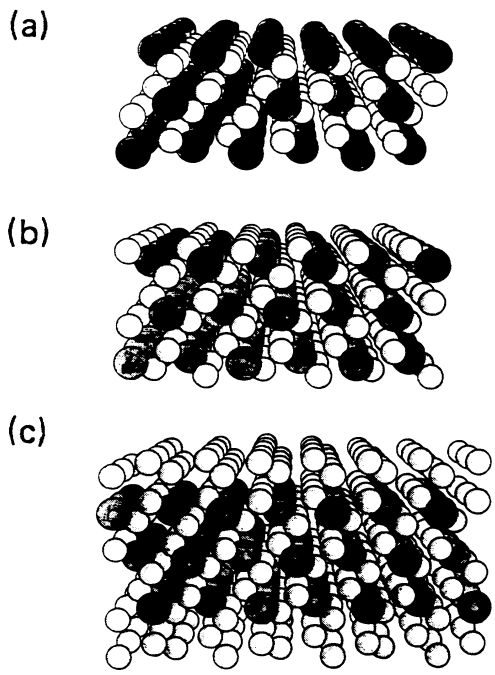

FIG. 5. Atomic slab models used for calculating electronic structure of $CoSi_2$(111) surfaces. (a) Cobalt-terminated $CoSi_2$(111), as suggested by Pirri *et al.* (Ref. 11) for the cobalt-rich surface. The outer Co atoms have four Si nearest neighbors. (b) Silicon-terminated $CoSi_2$(111), as suggested by Hellman and Tung (Ref. 12) for the cobalt-rich surface, with sevenfold-coordinated outer Co. (c) Hellman-Tung silicon-rich model, with eightfold-coordinated outer Co. The models have two-dimensional periodicity and inversion symmetry. They have three Co atoms and four, six, and ten Si atoms per unit cell, respectively. (View is from the side, with surface normal directed upwards. Co atoms are represented by the dark circles.)

In comparing these calculations to photoemission data we focus on the surface-state behavior observed for the cobalt-rich surface. Only the silicon-terminated model for the $CoSi_2$(111)-Co surface, with sevenfold coordination of the outer Co atoms, has a strong feature that corresponds to the surface state of Λ_1 symmetry at $\bar{\Gamma}$. The calculated surface state is marked in the band-structure diagram for this model (Fig. 6). It appears as two states marked 1 and 1′ (i.e., L_1 and L_1' symmetry) of different parity with respect to inversion because the model structure has two free surfaces. The charge density for these two states is concentrated at the surface Co atoms. The state localized on the top (or bottom) surface is an even (or odd) combination of the symmetrized bands; the near degeneracy of these bands in the neighborhood of $\bar{\Gamma}$ indicates that the two localized states are themselves nearly energy eigenstates and do not hybridize significantly through the intervening "bulklike" layers (four Si and one Co). This supports the identification of this band pair as a surface state of the bulk crystal. It is derived predominantly from the Co($3d_{z^2}$) orbital at the surface (z lies along [111], the surface normal), and is split from the bulklike bands below because the surface Co has one Si nearest neighbor in the $\pm z$ direction compared to two at bulk sites. In the calculations, the surface state and the related bulklike state lie 0.5 eV lower than observed experimentally, which is consistent with the pseudofunction

TABLE I. Bulk $CoSi_2$ band extrema for $CoSi_2$(100).

Band	ARUPS energy	LAPW[a]
X_1 bonding	-7.0 ± 0.2	-7.1
X_1 and X_5 nonbonding[b]	-2.0	$-2.0, -1.85$
Δ_5 bonding/Γ_{25}	-4.0 ± 0.2	-4.1 to -3.5
Γ_{12}	-1.9 (unclear)	-1.85

[a]Source: Ref. 6.

[b]The experimental geometry prevented the use of incidence-angle variation to distinguish between the $A_\perp$-sensitive X_1 and $A_\parallel$-sensitive X_5.

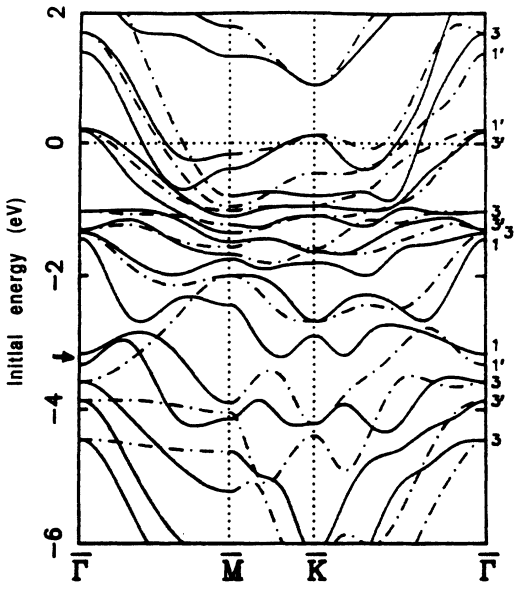

FIG. 6. Computed band structure for the silicon-terminated slab model of Fig. 5(b). Line styles indicate parity with respect to $(\bar{1}10)$ mirror plane along $\bar{\Gamma}-\bar{M}$, and with respect to C_2 axes along $\bar{M}-\bar{K}-\bar{\Gamma}$ (solid, even; dashed, odd). Labels at right denote symmetry of $\bar{\Gamma}$ states. The notation is that for L in the bulk Brillouin zone. (Point group D_{3d}: $L_1=A_g, L_1'=A_u, L_3=E_g, L_3'=E_u$.) The Λ_1 surface state (arrow) could be either L_1 or L_1'; the Λ_3 state, either L_3 or L_3'.

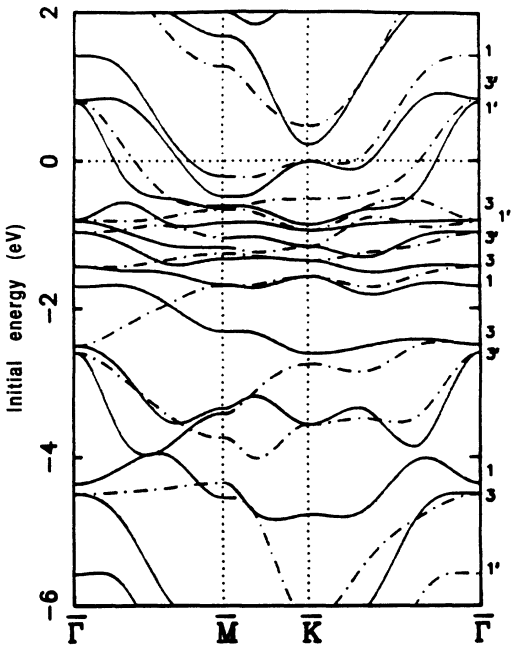

FIG. 7. Computed electronic band structure for the cobalt-terminated slab model of Fig. 5(a). Symmetry is indicated as in Fig. 6.

calculations of Co($3d$) bands for bulk $CoSi_2$ using the same basis functions.[19] As $\mathbf{k}$ increases away from $\bar{\Gamma}$ the computed surface state disperses upward. About one-third of the way from $\bar{\Gamma}$ to $\bar{M}$ or $\bar{K}$, the band gap in the projected band structure of bulk $CoSi_2$ (Ref. 6) closes up and, on a real (semi-infinite) $CoSi_2$ crystal, this state becomes a surface resonance. At this point the nearly degenerate curves in Fig. 6 separate. Continued upward dispersion of the resonance can be inferred from partial-density-of-states curves evaluated at surface and bulk Co atoms at different $\mathbf{k}_\parallel$ values, but accurate computation of this behavior requires calculations on thick model structures that exhibit clear bulklike behavior. The total dispersion of 1.2 eV from $\bar{\Gamma}$ to $\bar{M}$ agrees well with AR-UPS measurements (cf. Fig. 3), as does the behavior along most of the $\bar{\Gamma}-\bar{K}$ line.[11] In comparison, the cobalt-terminated model [Fig. 1(a)] cannot account for the Λ_1 surface state, since its band structure (Fig. 7) has no nearly degenerate pairs of states with the correct symmetry.

The band structure in Fig. 6 also accounts for the observed Λ_3 surface state about 0.3 eV above the nonbonding bulklike band. The state of L_3 symmetry at $\bar{\Gamma}$ that is concentrated on the center "bulklike" Co atom, and its band through the surface Brillouin zone, are lower than the corresponding surface-concentrated L_3 and $L_{3'}$ states and their bands. No region of near degeneracy between odd-parity and even-parity bands with respect to inversion is found. This agrees with the conclusion by Pirri *et al.* that this is a surface resonance rather than a true surface state.[11] The band structure also includes states nearer E_F related to bulk bands that account for structure near E_F in the off-normal-emission results seen in Fig. 3. While the relatively small basis set used in the calculations causes some inaccuracy in absolute energies, the essential surface electronic structure of the silicon-terminated model for the $CoSi_2$(111)-Co surface is in good agreement with the experimental results, whereas the cobalt-terminated model is not.

Since the $CoSi_2$(111)-Si surface is obtained from $CoSi_2$(111)-Co by adding two monolayers of Si atoms,[12] the above conclusion implies that the model of Fig. 1(b) is incorrect for $CoSi_2$(111)-Si, and that Fig. 1(d) or a variant with the same surface Si composition is correct. The band-structure results for this model (not shown) confirm that the Co($3d$)-derived states, which dominate the photoemission results discussed here, are indeed like those of bulk $CoSi_2$. Variations in the positions of the outer Si atoms should appear as changes in the Si-derived states which should appear stronger at lower photon energies. Those photoemission studies have not been performed in the present work.

IV. ELECTRONIC AND ATOMIC STRUCTURE OF THIN $CoSi_2$ FILMS ON Si(100)

$CoSi_2$ films were grown on Si(100) surfaces by depositing 2–3-Å Co onto a substrate at room temperature followed by heating to 460 °C. Most samples were prepared on silicon substrates cut and polished 4° off the (100) orientation (these are referred to as "off-axis" samples). Other films were prepared on a macroscopically rough substrate. Such substrates have been observed to yield

layers with large grains and sharp LEED patterns.[4] After ion bombardment cleaning and annealing, the substrates showed sharp (2×1) LEED patterns. The patterns for off-axis substrates showed a predominance of one domain orientation and clearly resolved splitting of most spots. LEED patterns for the rough substrate had an even mixture of (2×1) and (1×2) domains and showed no splitting. After Co deposition, no LEED patterns were visible. The samples were annealed at progressively higher temperatures, in ~10 °C steps, until the LEED pattern characteristic of $CoSi_2$ on Si(100) with a Co-rich surface[4] was observed. The temperature of silicide formation was measured to be 460 °C, in agreement with Yalisove *et al.*[4,5] LEED patterns from films grown on off-axis substrates did not have split spots like those of the clean substrate and appeared identical to those from films grown on macroscopically rough substrates. Thus the silicide film, about 7–9 Å thick, apparently removed the ordered array of double-layer steps that caused the spot splitting in the clean off-axis substrates.

The LEED pattern for these samples is illustrated schematically in Fig. 8(a), and can be described as a $p(2\times2)$ pattern in which the dominant beams describe a $(\sqrt{2}\times\sqrt{2})R45°$ pattern. The beams at $(1\,\frac{1}{2})$ are weak, but clearly visible; those at $(0\,\frac{1}{2})$ and at $(0\,\frac{3}{2})$ are not visible. A glide plane symmetry of the surface along the [011] directions accounts for the suppression of $[(0)(2k+1)/2)]$ beams.[20] A primary driving force that may explain the reconstruction is the large number of dangling bonds on a Si-terminated bulk $CoSi_2(100)$ surface [Fig. 8(b)]. The structure shown in Fig. 8(c), in contrast, has no Si dangling bonds and would account for the LEED pattern, although other structures are certainly possible. Here half a monolayer of Co is added and subsurface atoms are rearranged to allow the formation of Si dimers. Another interpretation of the LEED pattern is that the dominant phase has a $(\sqrt{2}\times\sqrt{2})R45°$ reconstruction, with smaller domains of a different structure that could account for the $(1\,\frac{1}{2})$ diffracted beams. Although there are plausible structures that would yield these additional spots,[19] scanning tunneling microscopy (STM) of $CoSi_2(100)$ films shows only domains with apparent $(\sqrt{2}\times\sqrt{2})R45°$ structure.[21] We note that the atomic positions in Fig. 8(b) deviate from $(\sqrt{2}\times\sqrt{2})R45°$ symmetry only in subsurface layers, and that the orientation difference between the bonding environments of atoms A and A' may produce no observable distinction in STM.

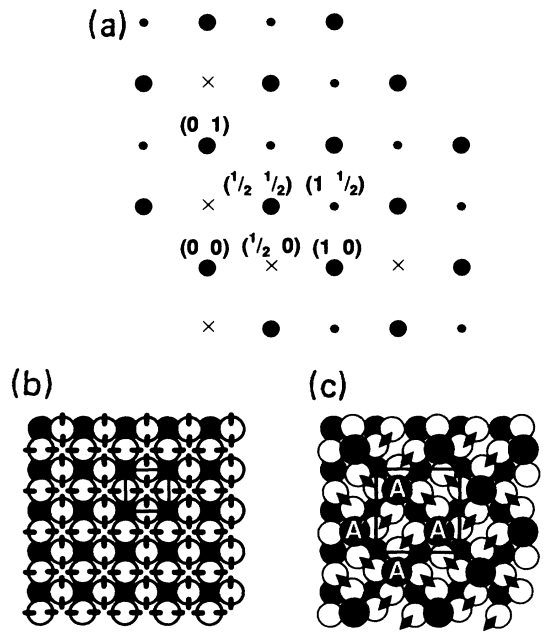

FIG. 8. LEED patterns and structural models for $CoSi_2(100)$. (a) LEED pattern characteristic of Co-rich $CoSi_2(100)$. Crosses mark missing spots which suggest glide-line symmetries. (b) Truncated-bulk model of $CoSi_2(100)$. Si atoms are light, Co atoms dark. Dark strokes denote Si dangling bonds, and the $p(1\times1)$ unit cell is marked by a box. (c) Suggested model of $CoSi_2(100)$ reconstruction. Dark diamonds denote Si–Si dimer bonds, and the $p(2\times2)$ unit cell is marked by a box. Cobalt atoms A and A' are equivalent by glide-line symmetry operation, but not by a pure translation.

Photoemission results show sensitivity of the film structure to details of preparation (Fig. 9). The first spectrum [9(a)] is characteristic of a high-quality layer as indicated by a sharp LEED pattern. The strongest feature is the $CoSi_2$ nonbonding peak which has a maximum at -1.35 eV. At about -2.5 eV there is a shoulder due to bulk emission from a Co($3d$) band of Δ_1 symmetry near Γ in the bulk Brillouin zone. A broad and diffuse swelling around -4 eV results from Co($3d$)-Si($3p$) bonding states in a band of Δ_5 symmetry. This feature is

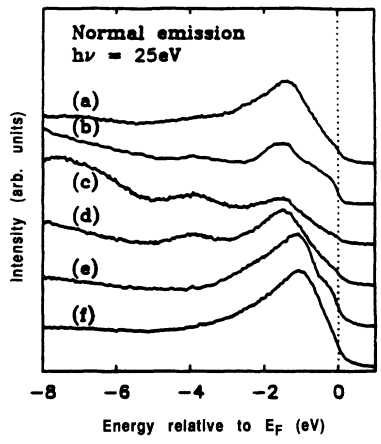

FIG. 9. Normal-emission photoemission spectra from various annealed layers of Co on Si(100). Photon energy is 25 eV and incidence angle is 70° from normal. (a) Template layer grown by depositing 2-Å Co and annealing at 450 °C. (b) Sputtered and annealed $CoSi_2(100)$ thick film. (c) 2-Å Co on Si(100), annealed >550 °C. Peak around -7 eV is from exposed Si after islands form. (d) Template layer with 3-Å Co, annealed 450 °C. (e) 4.5-Å Co, annealed 450 °C. (f) Unannealed room-temperature deposit of 1-Å Co/Si(100). The similarity between (e) and (f) suggests that kinetics of reaction limit the availability of Si to react with Co.

fairly weak because the photon polarization used here (polarization vector 20° from the surface normal) excites states of Δ_1 symmetry more strongly than Δ_5 states.

For comparison, spectra were collected from a $CoSi_2$ film ~100 Å thick of predominantly (100) orientation that was grown by the template method in a molecular-beam epitaxy (MBE) chamber, capped with Si for transfer into the photoemission chamber, ion-bombardment cleaned to expose $CoSi_2$, and annealed. A spectrum from this bulklike sample appears in Fig. 9(b). Some differences between Figs. 9(a) and 9(b), notably the increased intensity of bonding states, are due to a different experimental geometry (since at 45° angle of incidence photon polarization is 45° from normal, and the emission from Δ_5 states is increased). The nonbonding peak is somewhat different, as is confirmed in more surface-sensitive spectra: The peak in the bulklike spectrum appears more asymmetric and has a lower energy. The thin film's peak shape [Fig. 9(a)] corresponds to the sum of the bulklike $CoSi_2$ spectrum and a fairly strong surface component closer to E_F by ~0.3 eV. This upward shift of Co(3*d*) levels suggests that the Co atoms are not bonded to eight Si atoms at the surface as they are in the bulk. For this photon energy at least, the bulklike silicide has markedly more emission near the Fermi level than the template layer.

Small variations in film preparation cause marked changes in photoemission results. For a thin-layer sample annealed at about 550 °C, compared to 460 °C for the high-quality films, the form of the spectrum is similar in the Co(3*d*) energy region [Fig. 9(c)]. The nonbonding Co(3*d*) intensity relative to background is lower, however, and there is a strong feature at −7 eV due to the silicon density of states, suggestive of exposed Si regions. This agrees also with the LEED pattern of the sample, in which the $(0\,\frac{1}{2})$ spots of clean Si(100) have reappeared and the $(\frac{1}{2}\,\frac{1}{2})$ spots, dominant for other $CoSi_2$(100) samples, are relatively weak. The strength of the Co(3*d*) bonding peak could be due to increased scattering and reduced symmetry at boundaries between $CoSi_2$ and exposed Si. The spectrum in Fig. 9(d) comes from a sample whose initial Co deposit was 3 Å, not 2 Å. In most respects its LEED pattern and photoemission spectra are similar to those of the sample used for Fig. 9(a), but there is a marked increase in emission from the bonding peak. The LEED pattern includes streaking in the $[0\zeta]$ directions, which suggests an increase in structural disorder because of excess Co. Variation of sample annealing temperature may also play a role here, though for high-quality layers, the LEED pattern was not improved by raising the temperature after the pattern first appeared. When the initial Co coverage was increased further to 4.5 Å, the sample did not show the LEED pattern characteristic of ordered $CoSi_2$ films. The main peak in its spectrum [Fig. 9(e)] is quite similar to that obtained when 1-Å Co is deposited on Si(100) without annealing [Fig. 9(f)]. It seems that the spectrum in Fig. 9(e) is approximately a weighted superposition of Figs. 9(f) and 9(b). This is interpreted to indicate the presence of $CoSi_2$ underneath an incompletely reacted Co layer. This conclusion is in accord with the suggestion by Yalisove, Tung, and Batstone[4] that transport of Si through the $CoSi_2$ at 450 °C is the limiting step in the growth of $CoSi_2$ on Si(100). The spectra in Fig. 9 suggest that the sites of outer Co atoms in well-ordered layers, while not identical to those in bulk $CoSi_2$, are closer to bulklike than to that of unannealed Co on Si(100). The spectrum 9(a) resembles those of the Co-rich $CoSi_2$(111) surface which has Co atoms bonded to seven Si atoms (Sec. III B).

Photon-energy dependence at normal emission was measured for the MBE-grown $CoSi_2$(100) film (Figs. 10 and 11) and yields band extrema (Fig. 12) in close agreement with band-structure calculations (Table I). The data suggest the presence of surface states at −1.3 and −2.8 eV on the (100) surface ion cleaned and annealed at 650 °C. Normal-emission spectra from high-quality $CoSi_2$ films grown *in situ* show dispersive features that agree well with bulk $CoSi_2$(100) bands of (*sp*) character. Spectra at off-normal emission angles, on the other hand, do not reveal dispersion of the dominant Co(3*d*) peaks with $\mathbf{k}_\parallel$. This would not be surprising for a structure like that shown in Fig. 8(c) because of the large distance between surface Co atoms. The nearly isolated Co atoms and Si dimers in Fig. 8(c) would be characterized by localized bonds that would yield strong nondispersive contributions to photoemission. Surface Co(3*d*) states could still couple through hybridization with the bulk bands. However, the energies of Co(3*d*) atomic states in surface and bulk sites should differ considerably because of the

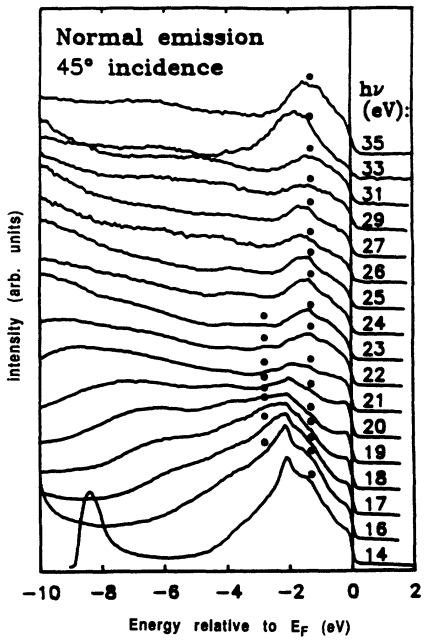

FIG. 10. Normal-emission photoemission spectra from bulklike $CoSi_2$(100) film, sputtered and annealed. Photon energy is varied from 14 eV to 35 eV. Peak variations among the spectra mostly indicate dispersion of bulk bands with $k_\perp$. The marked peaks are interpreted to arise from surface states. Incidence angle is 45°.

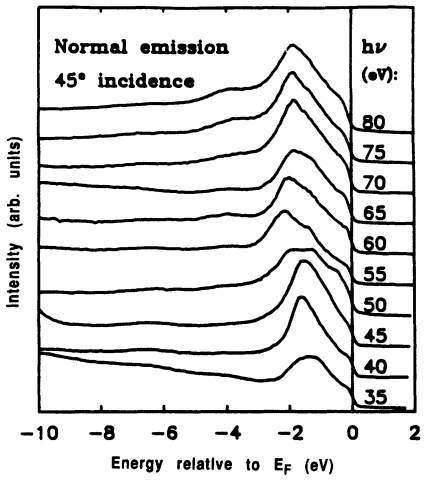

FIG. 11. Normal-emission photoemission spectra from bulk-like $CoSi_2$(100) film, at higher photon energies. Photon energy is varied from 40 to 80 eV. Incidence angle is 45°. Third-order diffracted beam from monochromator causes Si($2p$) core levels to appear below −10 eV in the 45-eV spectrum and below E_F in the 50-eV spectrum.

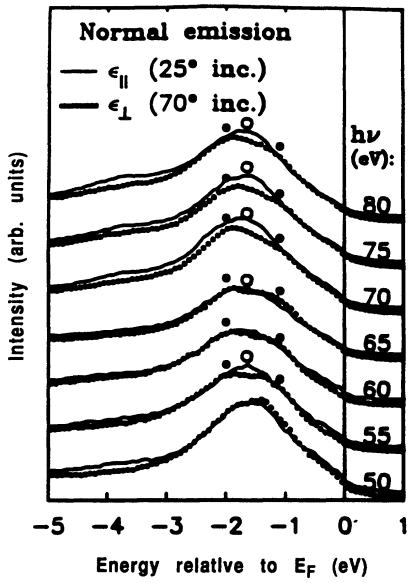

FIG. 13. Polarization dependence of surface-sensitive spectra from $CoSi_2$ "template" layer. Solid curves are for 25° incidence ($A_{\parallel}$ dominates); symbols show spectra for 70° incidence ($A_{\perp}$ dominates). Positions of three component peaks are shown at −2.0, −1.65, and −1.1 eV.

marked difference in bonding environment (4 vs 8 Si nearest neighbors), so the matrix elements for surface-bulk hybridization could be small. This contrasts with $CoSi_2$(111)-Co in which neighboring surface Co atoms have 2 Si nearest neighbors in common, and in which the similar surface and bulk bonding structures are more conducive to surface-bulk hybridization.

The polarization dependence of normal-emission spectra (Fig. 13) shows more variation than the dependence on emission angle. The peaks appear to consist of three main features. Two features at −1.8 to −2.0 eV and at −1.0 to −1.4 eV have Δ_1 symmetry, which indicates that normal emission is excited by the component of the vector potential normal to the surface $A_{\perp}$. (The ranges indicate variation between samples.) The third peak, at −1.65 eV, is sensitive to $A_{\parallel}$ and thus has Δ_5 symmetry. The deepest peak is close to the density-of-states maxima

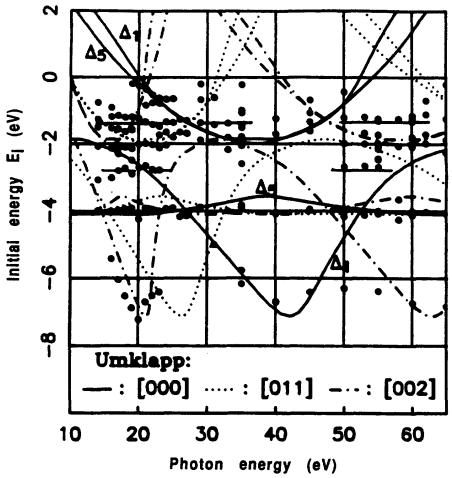

FIG. 12. Comparison of observed ARUPS peaks with calculated bulk-band dispersion. Bulk bands (Ref. 6) are converted into E_i-vs-$h\nu$ curves using a free-electron final-state assumption with inner potential $V_0 = 16.8$ eV. Different line styles denote different surface umklapp vectors, as marked. Horizontal lines suggest surface states at −1.3 and −2.8 eV.

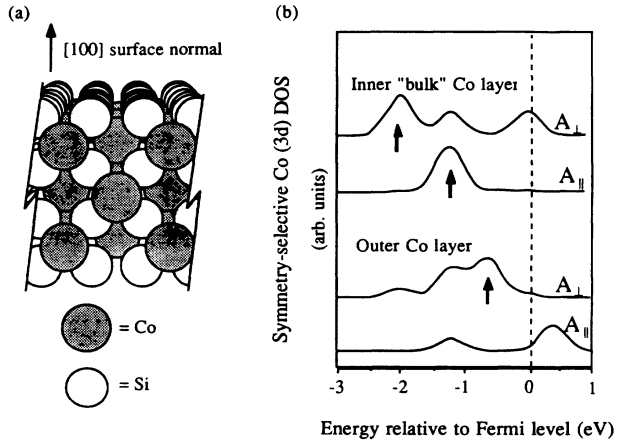

FIG. 14. Calculated Co states in nonbonding energy region for unreconstructed $CoSi_2$(100) surface. (a) Atomic model (viewed from side). (b) Symmetry- and $\mathbf{k}_{\parallel}$-selective local-density-of-states curves at inner ("bulk") and outer ("surface") Co atoms. These curves indicate which states can appear in normal photoemission with different photon polarization ($A_{\parallel}$ or $A_{\perp}$). Arrows indicate three states that appear to correspond to photoemission features.

for the X_1 and Γ_{12} nonbonding states in the bulk band structure derived from the Co($3d_{z^2}$) orbital, where z is the surface normal. The other two peaks may be surface peaks split off by the electronic difference between surface and bulk Co, with the $\Delta_1(d_{z^2})$ state around -1.2 eV and the $\Delta_5(d_{xz})$ state at -1.65 eV. The bulk $CoSi_2$ band structure has no band gap among the Δ_1 states in this energy range, so the state near -1.2 eV should be a surface resonance rather than a true surface state. Such a resonance couples to bulk propagating states so its energy in these films with only 3–4 Co layers depends on film thickness and on the structure of the buried interface. This holds also for the bulk Δ_1 state at -1.8 to -2.0 eV. The energy variations between samples can be satisfactorily explained by variations in film thickness. A comparison with computational analysis for the Co states in the nonbonding energy region for the unreconstructed $CoSi_2$(100) surface is shown in Fig. 14. These curves show which states can appear in normal photoemission with different photon polarizations. Three states corresponding to the observed photoemission features for the proposed model are indicated.

V. SUMMARY AND CONCLUSIONS

A. $CoSi_2$/Si(111) film structure

Combining ARUPS measurements with *ab initio* calculations of electronic structure leads to several significant conclusions about the behavior of Co on Si(111). The ARUPS results confirm that well-ordered $CoSi_2$(111) surfaces can be either cobalt rich or silicon rich, the latter being the more stable surface formed at higher temperatures. Photoemission from $CoSi_2$(111)-Si agrees with calculated bulk electronic structure, with no observed surface states. Our calculations show that removing even a single Si nearest neighbor from Co in $CoSi_2$ induces strong changes in the electronic structure. Thus the bulklike electronic structure observed in photoemission implies that surface Co atoms are in a bulklike bonding environment. The density of states of $CoSi_2$(111)-Co, on the other hand, is shown to be essentially that of $CoSi_2$(111)-Si plus a contribution from the surface Co atoms which lies at 0.7 eV higher energy. The behavior of the observed dispersive state on the cobalt-rich surface identifies as correct the silicon-terminated structure with sevenfold-coordinated Co on the outer layer as discussed in Sec. III B. The calculations show that the difference between sevenfold and eightfold coordination, though seemingly small, is sufficient to account for the electronic difference between silicon-rich and cobalt-rich $CoSi_2$(111) surfaces. The present work shows that the atomic models of Figs. 1(c) and 1(d), which had been based on several structure-sensitive probes, are also supported by measurements of valence-band *electronic* structure. In Sec. III B we compare the measured band dispersion for several surface states with structure-specific theoretical models. Although we do not suggest that this comparison is a unique structural determination, it does provide an important consistency test of the available structural models shown in Fig. 1.

B. $CoSi_2$/Si(100) film structure

$CoSi_2$ epitaxy on Si(100) is more complex and requires more extended consideration. Photoemission experiments indicate that "template" techniques produce films of fairly well-ordered silicide and that moderate deviations from optimal sample preparation recipes produce observably different films. Annealing at too high a temperature (550 °C vs 460 °C) yields exposed Si areas and produces poor templates for further growth. Excessive Co coverage produces underreacted Co near the surface. High-quality thin films, formed by annealing 2 Å Co at 450 °C, have an electronic structure that suggests that the outermost Co atoms are bonded to fewer than 8 Si neighbors. The detailed structure, however, is yet to be determined. The model structure presented in Fig. 8 accounts for the LEED pattern, STM images, and, qualitatively, photoemission results. However, this model admittedly may not be unique. Additional studies on the detailed structure of initial silicide layers will be needed to optimize the sample preparation by improving the performance of the cobalt- and silicon-vapor sources and by using all available empirical information on the relationship of template formation to the final film structure. When films of controlled uniform thickness can be grown, the changes in the energies of nonbonding Δ_1 states with increasing $CoSi_2$ film thickness are expected to yield important information on the surface structure and on the electronic properties of the interface. Analyzing these data will be facilitated by comparison with accurate band-structure calculations for specific film thicknesses.

The major goal of these studies is to achieve an improved understanding of the chemical physics of Co-Si reactions. In particular, the results help to explain why high-quality $CoSi_2$ epitaxy is much more difficult to achieve on Si(100) than on Si(111). The structures of both "Co-rich" and "Si-rich" $CoSi_2$, as well as of Si(111)/$CoSi_2$(111) interfaces, suggest an energy preference for configurations in which Co is bonded to as many as 7 or 8 Si atoms, even if some Si atoms do not have their full fourfold bond complement. On a $CoSi_2$(100) surface a bulklike Co environment can occur only with many Si dangling bonds or with highly distorted surface bonds. The structure proposed in Fig. 8(c) abandons the constraint of nearly full bonding for surface Co. It may be regarded as bulk $CoSi_2$ truncated above a Si plane with 0.5 ML of Co adatoms serving to satisfy Si dangling bonds. Geometric constraints also make it difficult to achieve full Co-Si coordination at the Si(100)/$CoSi_2$(100) interface. It remains to achieve a complete determination of the $CoSi_2$(100) surface and interface structures, and to perform systematic computational studies of the total energies of different structures. With that information about formation of these structures, definition of the required chemical and structural treatments of the Si(100) surface can be most useful to overcome difficulties in producing high-quality silicide epitaxy for the Si(100)/$CoSi_2$(100) interface using the template approach.

ACKNOWLEDGMENTS

The experimental work was conducted at the National Synchrotron Light Source, Brookhaven National Laboratory, supported by the U.S. Department of Energy, Division of Materials Sciences and Division of Chemical Sciences (DOE Contract No. DE-AC02-76CH00016). Research support by the Materials Science Center at Cornell University Grant No. (NSF-DMR8818558) and computational support from the Cornell National Supercomputer Facility (Theory and Simulation Center Grant No. NSF-ASC8500641) are acknowledged. We thank R. Kasowski for the use of his computer programs, and S. Yalisove, R. Tung, K-L Tsang, Z. Lin, W. O'Brien, P. Tangyunyong, and R. Ozer for help with experiments.

---

*Present address: IBM Research Division, Almaden Research Center, 650 Harry Road, San Jose, CA 95120.

[1]J. Derrien and F. Arnaud d'Avitaya, J. Vac. Sci. Technol. A **5**, 2111 (1987).

[2]J. C. Bean and J. M. Poate, Appl. Phys. Lett. **37**, 643 (1980); K. C. R. Chiu, J. M. Poate, J. E. Rowe, T. T. Sheng, and A. G. Cullis, Appl. Phys. Lett. **38**, 988 (1981); H. Ishiwara, in *Proceedings of the Symposium on Thin Film Interfaces and Interaction,* edited by J. E. Baglin and J. M. Poate (Electrochem. Soc., Pennington, NJ, 1980); S. Saitoh, H. Ishiwara and S. Furukawa, Appl. Phys. Lett. **37**, 203 (1980).

[3]C. W. T. Bulle-Lieuwma, A. H. van Ommen, and J. Hornstra, in *Epitaxy of Semiconductor Layered Structures,* edited by R. T. Tung, L. R. Dawson, and R. L. Gunshor, MRS Symposia Proceedings No. 102 (Materials Research Society, Pittsburgh, 1988), p. 377.

[4]S. M. Yalisove, R. T. Tung, and J. L. Batstone, in *Heteroepitaxy on Silicon: Fundamentals, Structures, and Devices,* edited by H. K. Choi, R. Hull, H. Ishiwara, and R. J. Nemanich, MRS Symposia Proceedings No. 116 (Materials Research Society, Pittsburgh, 1988), p. 439.

[5]S. M. Yalisove, R. T. Tung, and D. Loretto, J. Vac. Sci. Technol. A **7**, 1472 (1989).

[6]L. F. Mattheiss and D. R. Hamann, Phys. Rev. B **37**, 10623 (1988).

[7]W. R. L. Lambrecht, N. E. Christensen, and P. Blöchl, Phys. Rev. B **36**, 2493 (1987).

[8]G. C. F. Newcombe and G. G. Lonzarich, Phys. Rev. B **27**, 10619 (1988).

[9]G. Gewinner, C. Pirri, J. C. Peruchetti, D. Bolmont, J. Derrien, and P. Thiry, Phys. Rev. B **38**, 1879 (1988).

[10]C. Pirri, G. Gewinner, J. C. Peruchetti, D. Bolmont, and J. Derrien, Phys. Rev. B **38**, 1512 (1988).

[11]C. Pirri, J. C. Peruchetti, D. Bolmont, and G. Gewinner, Phys. Rev. B **33**, 4108 (1986).

[12]F. Hellman and R. T. Tung, Phys. Rev. B **37**, 10786 (1988).

[13]B. D. Hunt, N. Lewis, E. L. Hall, L. G. Turner, L. J. Scholwalter, M. Okamoto, and S. Hashimoto, in *Layered Structures and Epitaxy,* edited by J. M. Gibson, G. C. Osborn, and R. M. Tromp, MRS Symposia Proceedings No. 56 (Materials Research Society, Pittsburgh, 1986), p. 151.

[14]J. Vrijmoeth, A. G. Schins, and J. F. van der Veen (unpublished).

[15]S. A. Chambers, S. B. Anderson, H. W. Chen, and J. H. Weaver, Phys. Rev. B **34**, 913 (1986).

[16]R. Leckey, J. D. Riley, R. L. Johnson, L. Ley, and B. Ditchek, J. Vac. Sci. Technol. A **6**, 63 (1988) ; J. E. Rowe, G. K. Wertheim, and R. T. Tung, *ibid.* 7, 2454 (1989).

[17]R. V. Kasowski, T. N. Rhodin, M. -H. Tsai, and D. D. Chambliss, Phys. Rev. B **34**, 2656 (1986).

[18]M. -H. Tsai, R. V. Kasowski, and T. N. Rhodin, Surf. Sci. **179**, 143 (1987); M. -H. Tsai, J. D. Dow, and R. V. Kasowski, Phys. Rev. B **38**, 2176 (1988).

[19]D. D. Chambliss, Ph. D. thesis, Cornell University, 1989.

[20]B. W. Holland and D. P. Woodruff, Surf. Sci. **36**, 488 (1973).

[21]R. Becker (private communication).

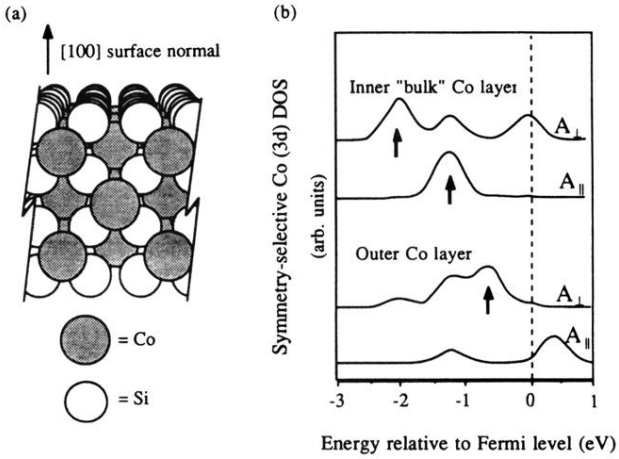

FIG. 14. Calculated Co states in nonbonding energy region for unreconstructed $CoSi_2(100)$ surface. (a) Atomic model (viewed from side). (b) Symmetry- and $\mathbf{k}_\parallel$-selective local-density-of-states curves at inner ("bulk") and outer ("surface") Co atoms. These curves indicate which states can appear in normal photoemission with different photon polarization ($A_\parallel$ or $A_\perp$). Arrows indicate three states that appear to correspond to photoemission features.

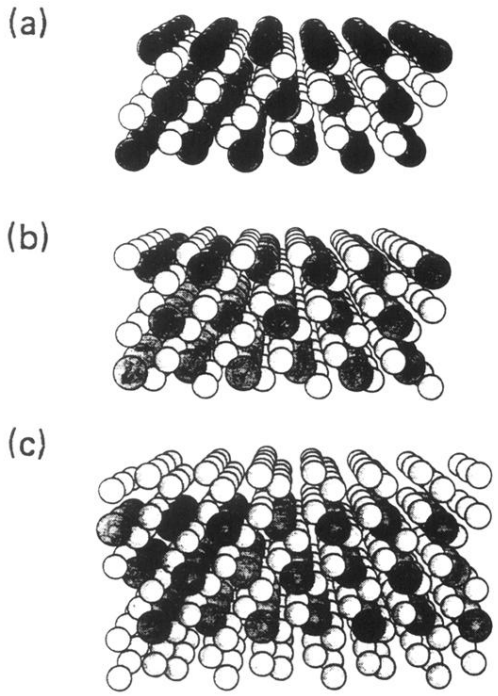

FIG. 5. Atomic slab models used for calculating electronic structure of $CoSi_2(111)$ surfaces. (a) Cobalt-terminated $CoSi_2(111)$, as suggested by Pirri *et al.* (Ref. 11) for the cobalt-rich surface. The outer Co atoms have four Si nearest neighbors. (b) Silicon-terminated $CoSi_2(111)$, as suggested by Hellman and Tung (Ref. 12) for the cobalt-rich surface, with sevenfold-coordinated outer Co. (c) Hellman-Tung silicon-rich model, with eightfold-coordinated outer Co. The models have two-dimensional periodicity and inversion symmetry. They have three Co atoms and four, six, and ten Si atoms per unit cell, respectively. (View is from the side, with surface normal directed upwards. Co atoms are represented by the dark circles.)